Int. J. Electrochem. Sci., 13 **(2018)** 11882 – 11894, doi: 10.20964/2018.12.85

International Journal of
ELECTROCHEMICAL
SCIENCE
www.electrochemsci.org

Corrosion Behaviour of a Zn/Zn-Al Double Coating in 5% NaCl Solution

Tian-yu Weng, Gang Kong[*]*, Chun-shan Che, Yan-qi Wang*

School of Material Science and Engineering, South China University of Technology, Guangzhou 510640, China
[*]E-mail: sub_corrosion@163.com

Received: 8 September 2018 / *Accepted:* 16 October 2018 / *Published:* 5 November 2018

A new hot dip-galvanized Zn/Zn-5Al double coating was prepared by immersing steel into a molten pure zinc bath and then in a Zn-5Al alloy bath. The corrosion behaviour of the double coating was studied in 5% NaCl solution. The results showed that the coating consisted of a typical coating of Zn on the bottom with a Zn-Al layer on the top. The maximum thickness of the alloy coating was approximately 220 μm. The neutral salt spray (NSS) test showed that the double coating was significantly effective for preventing corrosion. The corrosion resistance of the Zn-5Al alloy-coated steel was almost four times that of the Zn-coated steel according to the NSS test. The electrochemical tests indicated that the corrosion resistance of the Zn/Zn-Al double coating decreased with immersion time. However, the double coating also had a higher corrosion resistance and more negative corrosion potential compared with Zn-coated steel in 5% NaCl solution. SEM and XRD analyses revealed that the improved corrosion resistance of the Zn/Zn-5Al double coating was mainly due to the effect of Al on the corrosion products on the coating surface.

Keywords: hot-dip Zn-5Al coating; EIS; corrosion.

1. INTRODUCTION

Corrosion protection of steel is usually achieved by hot-dip galvanizing, which enables steel to be applicable as the most important material for automotive, construction and household appliance industries [1-8]. In the past few decades, to improve the corrosion resistance of zinc-based coatings, a large effort has been undertaken to adding some alloying elements, e.g., aluminium, magnesium, cobalt, nickel, manganese, and tin, to the molten zinc bath [3, 9-11]. Among these alloying elements, the addition of Al to molten zinc bath has been widely used in industry to obtain Zn-Al alloy coatings. The corrosion behaviour of Zn-Al alloy coatings under atmospheric environments containing chloride

ions has been widely studied, and all researchers agree that the addition of Al enhances the corrosion resistance of Al-containing coatings [12-28]. In addition, the presence of alloying Al in the Zn bath can limit the zinc–iron reactivity and improve the bath fluidity of zinc-based coatings [3, 11]. The conventional hot-dip Zn-5Al coating is often very thin, although the corrosion resistance of the Zn-5Al coating is several times that of a pure zinc coating [3, 11]. It is necessary to increase the thickness of the Zn-5Al alloy coating to prolong the protection life of the Zn-5Al alloy coating for steel.

In the paper, to obtain a double Zn-5Al alloy coating with a thickness of more than that of the conventional hot-dip Zn-5Al coating, a new hot dip Zn-5Al alloy coating was made by dipping steel into a molten pure zinc bath and then immersing it into a Zn-5Al alloy bath. The corrosion resistance of the double coating was evaluated by open-circuit potential (OCP), electrochemical impedance spectroscopy (EIS), neutral salt spray (NSS) tests and potentiodynamic polarization curves. Scanning electron microscopy (SEM), energy dispersive X-ray spectroscopy (EDS) and X-ray diffraction (XRD) were used to characterize the corrosion products.

2. EXPERIMENTAL

The pre-coated steel was first immersed in a hot 10 wt.% NaOH solution for degreasing and in a 10 vol.% HCl solution to remove surface oxides; then, it was coated with $ZnCl_2$ + NH_4Cl for flux treatment. The Zn-Al alloys were prepared in a crucible resistance furnace with an Al ingot (purity of 99.996%) and a Zn ingot (purity of 99.995%). An argon shield was used when adding Al using a graphite rod to place Al ingots into the zinc bath at 670 °C; then, the alloy bath was incubated for 4 h at 540 °C after the Al ingots were melted in the zinc bath. The Zn-5Al alloy was coated onto the pre-treated steel via a double coating process: the first coating was performed by dipping into a molten zinc bath of 450 ± 5 °C, followed by immersion into a Zn-5Al alloy bath at 400 ± 5 °C. The dipping time into the zinc bath was 60 s. To ensure controllability and repeatability of the experimental results, the minimum immersion time in the Zn-5Al bath was 5 s. The obtained maximum thickness of the Zn/Zn-5Al double coating was approximately 220 μm after 5 s of immersion in the Zn-Al bath.

Table 1 Composition (%) of the steel used in this study

C	Cr	Mn	Ni	Si	P	S	Cu	Fe
0.054	0.075	0.168	0.04	<0.005	0.001	<0.001	0.017	Balance

A Zn/Zn-5Al double coating with a thickness of approximately 220 μm was used as the sample to evaluate its corrosion resistance in this study. Electrochemical tests were performed in a static 5% NaCl solution using a CHI660E potentiostation. A platinum sheet that was 5 cm^2 in size was used as the counter electrode. The reference electrode was a saturated calomel electrode (SCE). The working electrode area that was exposed to the NaCl solution was 2 cm^2. EIS spectra were collected in a frequency range of 10^5 Hz to 10^{-2} Hz at a corrosion potential with an amplitude of 5 mV. The impedance data were then analysed using ZSimpWin software. The open-circuit potential (OCP) was

obtained as a function of immersion time at regular intervals of up to 45 days of immersion. Potentiodynamic polarization curves were measured with a scan rate of 0.1 mV/s. The mass loss test was performed via the neutral salt spray (NSS) test (ASTM B117-18).

The morphology and elemental composition of the corrosion products were characterized by scanning electron microscopy (SEM) and a Quanta 200 microscope for energy dispersive X-ray spectroscopy (EDS), respectively. X-ray diffraction (XRD) was also used to characterize the corrosion products using Cu K_α radiation with an angular resolution of 0.02°, a counting time of 0.1 s/step, and an angular range of 10-80° (2θ).

3. RESULTS

3.1. Microstructure of the Zn/Zn-5Al double coating

Figure 1 shows the SEM images of the Zn/Zn-5Al double coating, a typical Zn-5Al coating and a Zn coating. Figure 1a shows that a thickness of approximately 220 μm for the Zn/Zn-5Al double coating could be obtained within the experimental parameters. This result indicates that the thickness of the Zn-5Al coating could be significantly increased by our dipping method. In Fig. 1a, it appears that the Zn-5Al layer replaced the pure Zn layer in Fig. 1c after 5 s of immersion in the Zn-5Al bath. The Zn-Al layer has a thickness of approximately 25 μm, and the Zn layer has a thickness of approximately 220 μm. The EDS analysis shown in Fig. 1d shows that the Zn-Al layer was composed Zn and Al with a mass ratio of 6.9: 93.1, which is very close to the designed bath composition. In addition, the XRD analysis in Fig. 1e also indicates that the double coating consisted of Zn and Al.

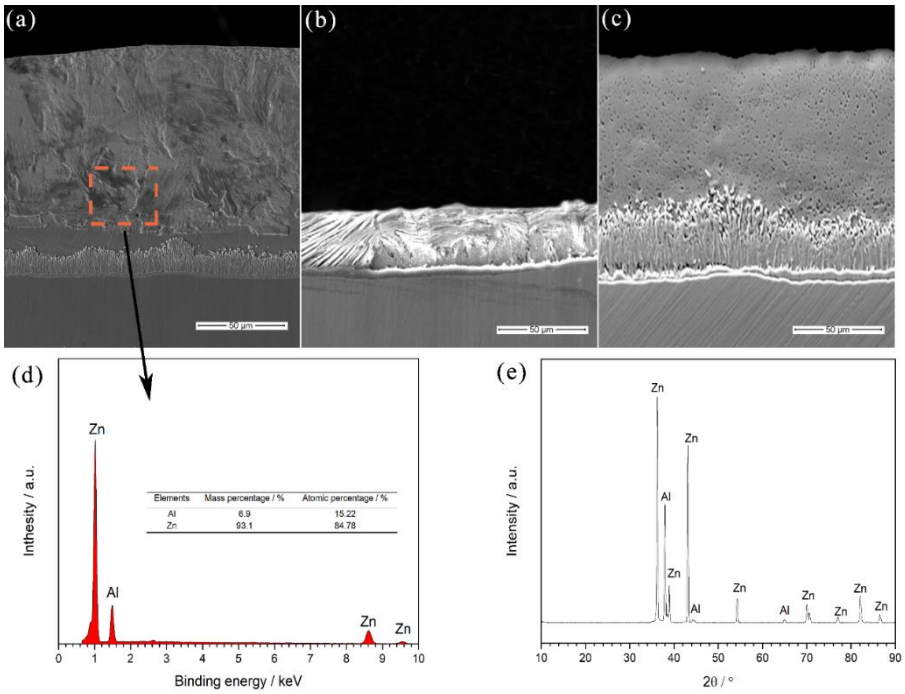

Figure 1. SEM images of a) a typical Zn/Zn-5Al double coating after 5 s of immersion, b) a typical Zn-5Al coating, and c) Zn coating before immersion in the Zn-5Al bath; d) EDS analysis for Fig. 1a and e) XRD pattern for Fig. 1a

3.2. Mass loss test

Figure 2 shows the mass losses of the Zn coating and the Zn/Zn-5Al double coating obtained from the neutral salt spray (NSS) test. As shown in Fig. 2, the mass loss of the Zn coating is 4-5 times larger than that of the Zn/Zn-5Al double coating. This result implies that the corrosion resistance of the Zn/Zn-5Al double coating was 4-5 times higher than that of the Zn coating. A previous study also reported that the corrosion resistance of a Zn-5Al coating was 3-5 times higher than that of a Zn coating. The result in the paper is consistent with previous studies [12, 16, 18, 19, 23].

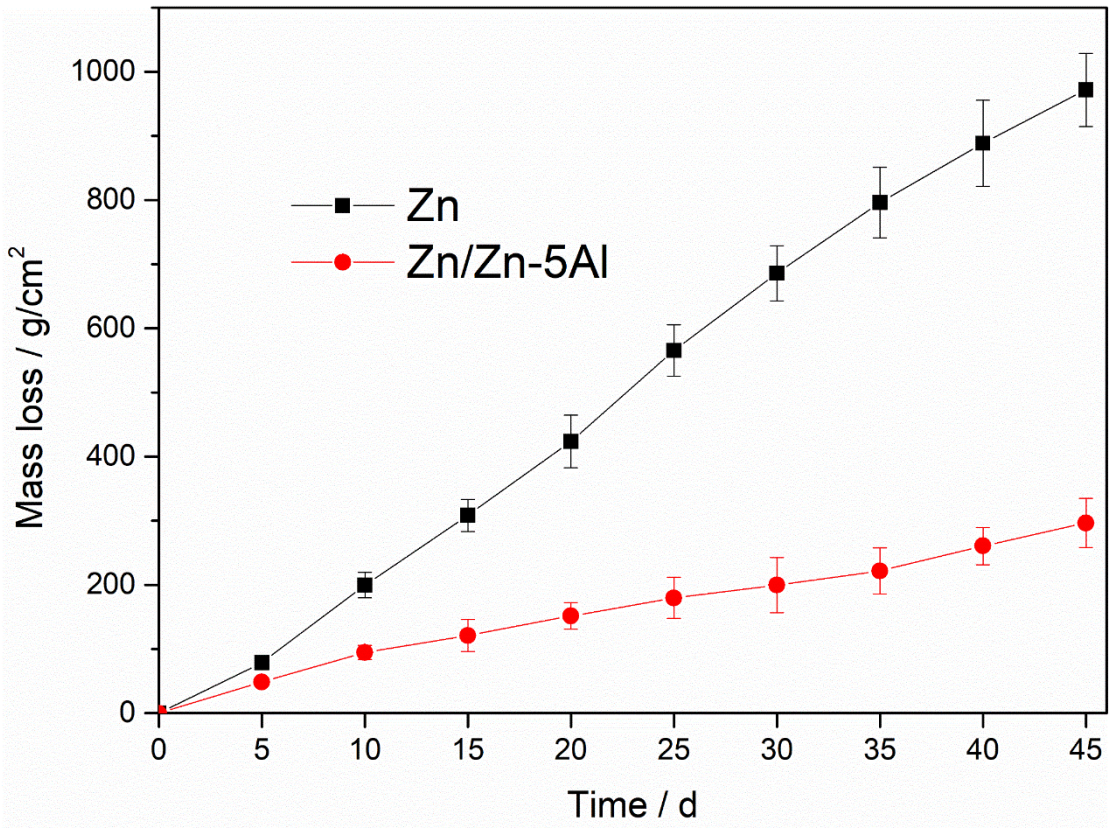

Figure 2. Mass loss of the Zn coating and the Zn/Zn-5Al coating as a function of time obtained by the neutral salt spray (NSS) test

3.3. Electrochemical study

Figures 3 shows the evolution of the OCP for the Zn coating and the Zn/Zn-5Al double coating as a function of immersion time in 5% NaCl solution. Figure 3 shows that the Zn/Zn-5Al double coating has more negative OCP than that of the Zn coating according to the immersion test. In addition, the OCP shifts to a positive direction with immersion time both for the Zn and Zn/Zn-5Al double coatings. However, the change in OCP for both the Zn and Zn/Zn-5Al double coatings is slight after 15 days of immersion. This result reveals that the Zn/Zn-5Al double coating has a better cathodic protection for steel than the Zn coating.

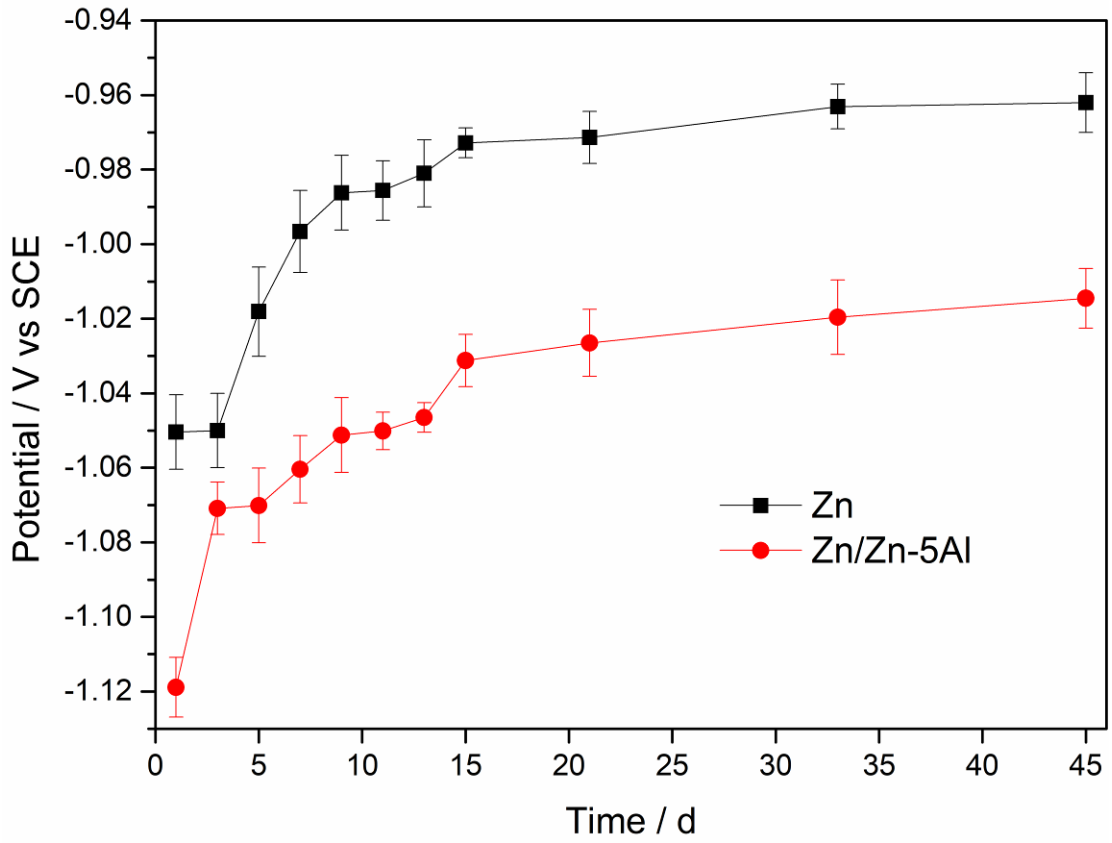

Figure 3. Change in the OCP for the Zn coating and the Zn/Zn-5Al double coating as a function of immersion time in 5% NaCl solution

The electrical equivalent circuit model illustrated in Fig. 4 was used to fit the EIS spectra. In the EC2 model, R_s is the solution resistance, Q is the constant phase element related to the interface phenomenon, and R is the charge-transfer resistance. The Warburg impedance (Z_w), a diffusional element in the low frequency region (in series with R), was introduced in the EC2 model. In the EC1 model, R_s corresponds to the solution resistance, where Q_1 and R_1 represent the capacitance and resistance of the phosphate coating, respectively, and Q_2 and R_2 represent the double layer capacitance and the charge transfer resistance of the metal/solution interface, respectively.

Figure 5 shows representative EIS spectra for the Zn coating after one day, 11 days and 45 days of immersion in 5% NaCl solution. In Fig. 5, at high frequencies, all Nyquist plots exhibit approximately a semicircle curve, which corresponds to a charge-transfer resistance (R) followed by a Warburg type impedance (Z_w). The electrical equivalent circuit model, EC2, shown in Fig. 4b was used to fit the EIS data in Fig. 5, which gave a satisfactory result. The fitting results are listed in Table 2.

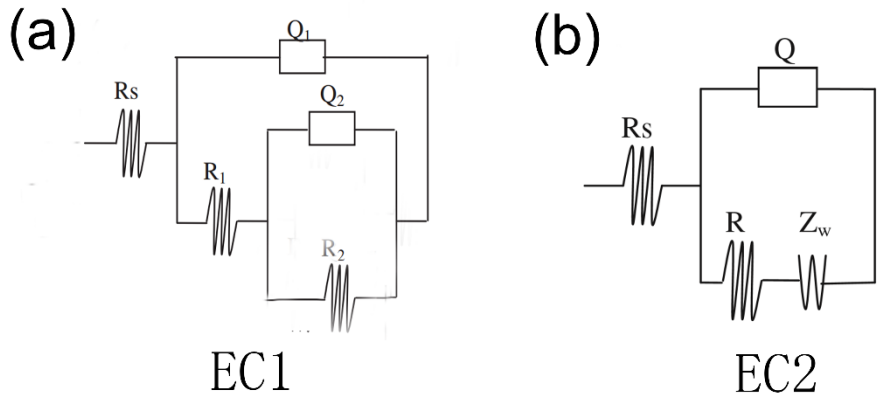

Figure 4. Equivalent circuit models used to fit the EIS diagrams

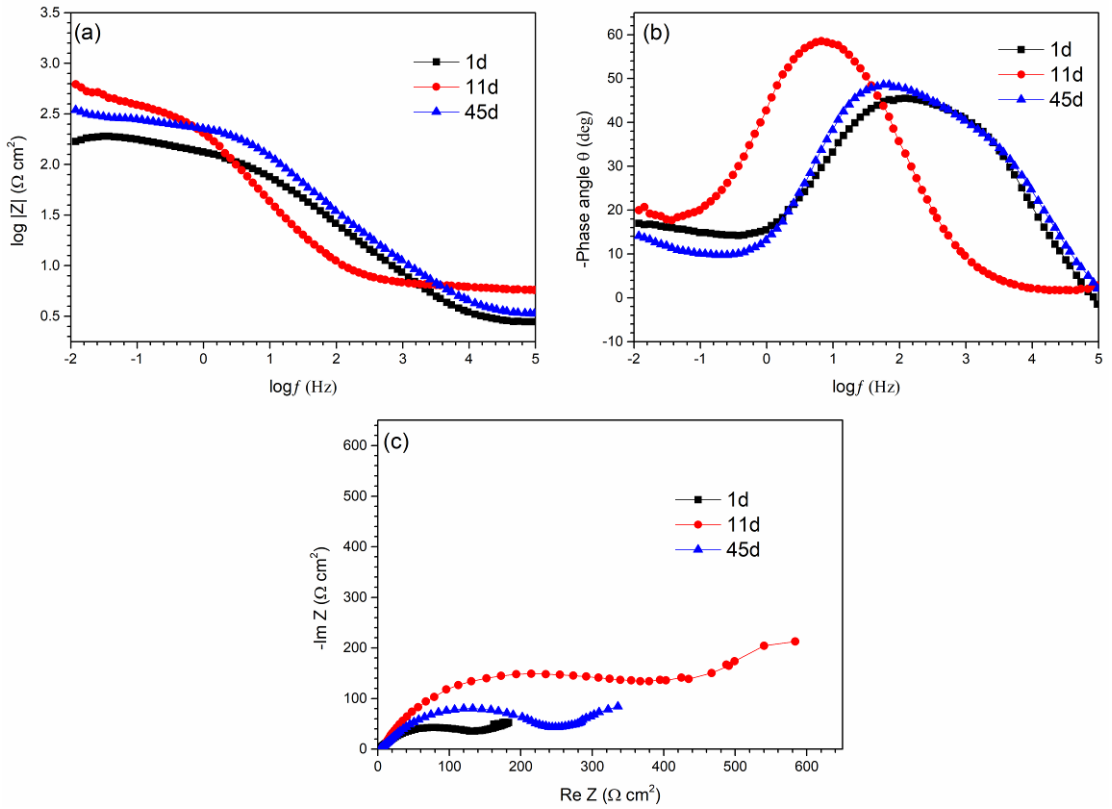

Figure 5. Bode diagrams and Nyquist spectra of the EIS measurements for the Zn coating in 5% NaCl solution

Figure 6 presents representative EIS spectra for the Zn/Zn-5Al double coating after one day, 11 days and 45 days of immersion in 5% NaCl solution. The EIS curves in Fig. 6 show two semicircles, which are not well defined. The electrical equivalent circuit model, EC1, shown in Fig. 4a was used to fit the EIS data in Fig. 6, which gave a satisfactory result. The fitting results are listed in Table 2.

The impedance in the low frequency end of the spectrum ($Z_{f\rightarrow 0}$) is usually interpreted as the polarization resistance, which is inversely proportional to the corrosion rate, i.e., the higher the

polarization resistance, the better the corrosion resistance. The polarization resistance can also be obtained by the sum of R_1 + R_2, and if there is one resistance that is the charge-transfer resistance, R_p is equal to the charge-transfer resistance.

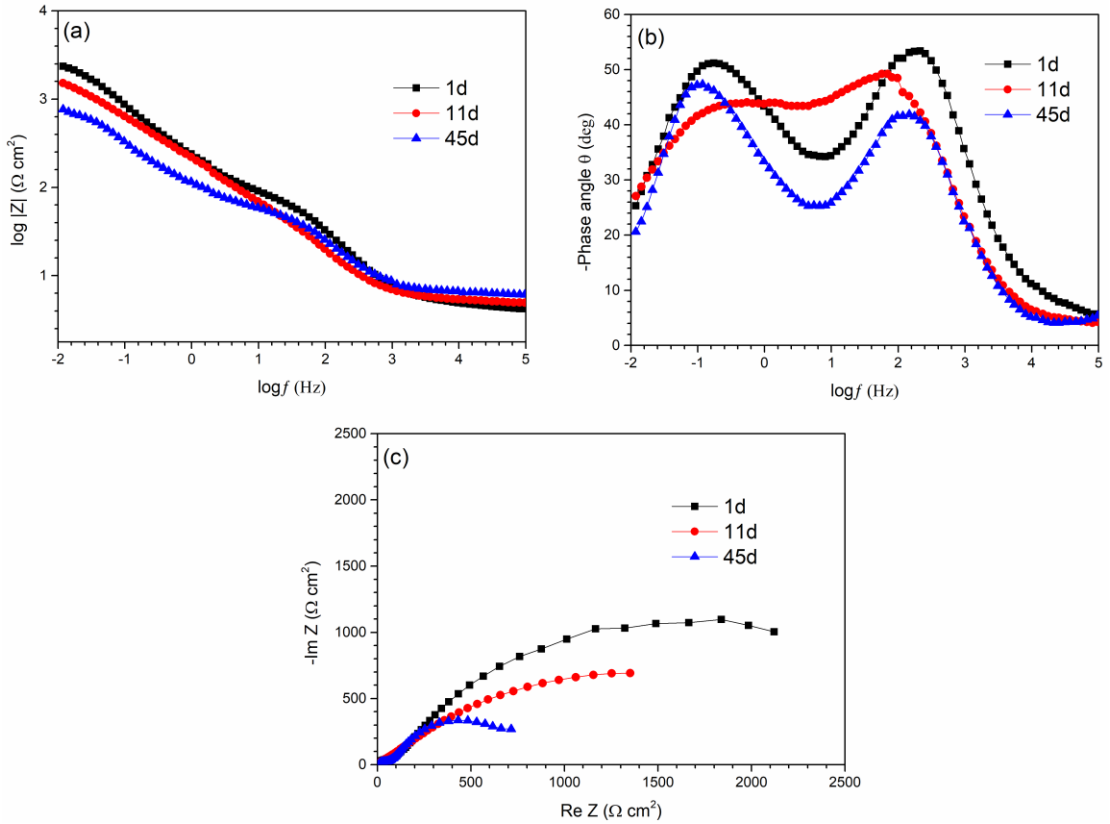

Figure 6. Bode diagrams and Nyquist spectra of the EIS measurements for the Zn/Zn-5Al double coating in 5% NaCl solution

Table 2. Fitting results of the EIS spectra of the Zn coating and the Zn/Zn-5Al double coating obtained from Figs. 6-7

Sample	Immersion time	R_s (Ω cm^2)	R_1/R (Ω cm^2)	n_1	Q_1-Y_0 (mS s^n cm^{-2})	R_2 (Ω cm^2)	n_2	Q_2-Y_0 (S s^n cm^{-2})	Z_w (Ω cm^2)	R_p (Ω cm^2)
Zn	1 d	3.1	269.30	0.64	0.436	-	-	-	0.036	269.34
Zn	11 d	4.1	386.40	0.79	0.892	-	-	-	0.014	386.41
Zn	45 d	3.8	153.00	0.62	0.665	-	-	-	0.040	153.04
Zn/Zn-5Al	1 d	4.5	107.50	0.81	0.169	3399.00	0.72	1.34	-	3506.50
Zn/Zn-5Al	11 d	5.1	97.37	0.75	0.431	2936.10	0.65	1.54	-	3033.47
Zn/Zn-5Al	45 d	4.3	63.96	0.74	0.262	1043.21	0.70	3.88	-	1107.17

As shown in Table 2, the value of R_p for the Zn/Zn-5Al double coating is approximately 10 times great than that for the Zn coating for different immersion times. This result indicates that the

Zn/Zn-5Al double coating has a higher corrosion resistance compared with the Zn coating, which is in good agreement with the result obtained from the mass loss test as shown in Fig. 2. Again, as shown in Table 2, for the Zn coating, the R_p increases from one to 11 days of immersion and then decreases after 11 days of immersion. For the Zn/Zn-5Al double coating, the R_p decreases with a prolonged immersion time.

Figure 7 shows representative polarization curves for the Zn coating and the Zn/Zn-5Al double coating after 45 days of immersion in 5% NaCl solution. The corrosion potentials and corrosion currents, I_{corr}, for the Zn coating and the Zn/Zn-5Al double coating were obtained by the Tafel extrapolation method. The corrosion potentials of the Zn coating and the Zn/Zn-5Al double coating were -1.04 V and -1.12 V vs. SCE, respectively. The corrosion currents, I_{corr}, of the Zn coating and the Zn/Zn-5Al double coating were 9.8 $\times 10^{-6}$ A/cm^2 and 5.5 $\times$ 10^{-5} A/cm^2, respectively. These results reveal that the Zn/Zn-5Al double coating had a more negative corrosion potential compared with that of the Zn coating in 5% NaCl solution. This is in good agreement with the result obtained from the OCP study in Fig. 3. In addition, the polarization curves in Fig. 7 indicate that Zn/Zn-5Al double coating had a higher corrosion resistance compared with the Zn coating. This result is in good agreement with that obtained in the EIS study shown in Table 2.

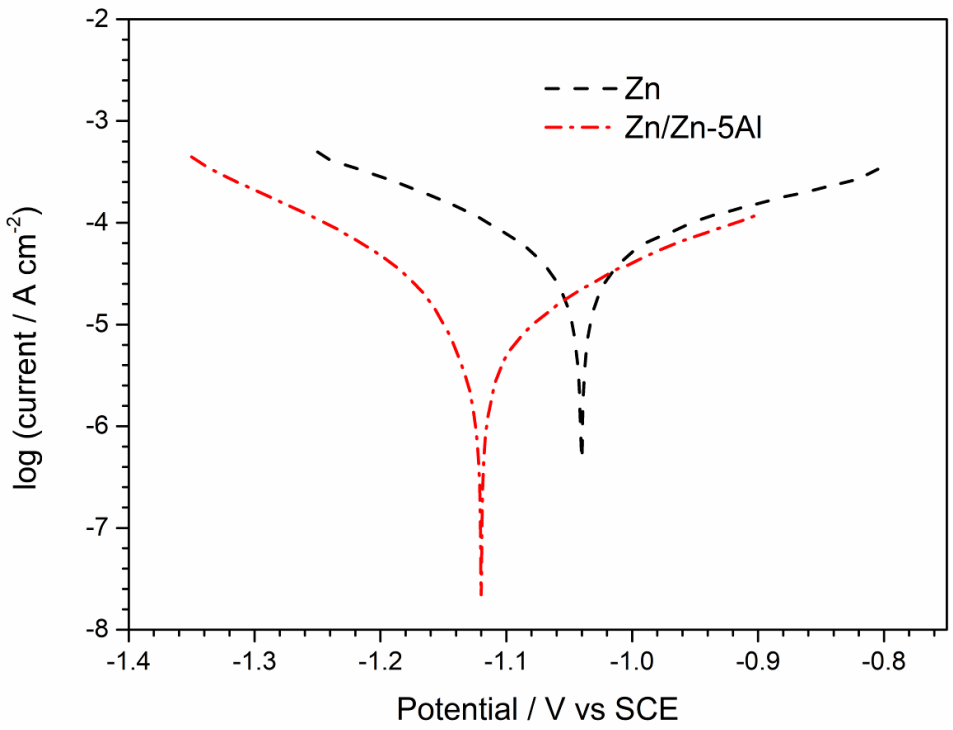

Figure 7. Representative polarization curves for the Zn coating and the Zn/Zn-5Al double coating after 45 days of immersion in 5% NaCl solution

3.4. Characterization of the corrosion products

Figure 8 depicts the SEM morphology of the corrosion products on the Zn coating and the EDS analysis of the corrosion products after 45 days of immersion in 5% NaCl solution. As shown in Figs.

8a-c, the entire coated surface was mainly covered with one kind of corrosion product layer after 45 days of immersion in 5% NaCl solution. The EDS analysis in Fig. 8d shows that the corrosion products mainly consisted of Zn, O and C. Figure 9 shows the SEM morphology of the corrosion products formed on the Zn/Zn-5Al coating and the EDS analysis of the corrosion products after 45 days of immersion in 5% NaCl solution. As shown in Figs. 9a-c, the entire coated surface was mainly covered by two kinds of corrosion product layers, i.e., a dark grey area and a main grey area. The SEM morphology of the dark grey area in Fig. 9b is similar to that of the Zn coating shown in Figs. 8b-c. EDS analysis also showed that the corrosion products mainly consisted of Zn, O and C (not shown here). However, the SEM morphology of the main grey area in Fig. 9c is quite different from that of the dark grey area. The EDS analysis shown in Fig. 9d indicates that the corrosion products mainly consisted of Zn, O, C, Cl and Al.

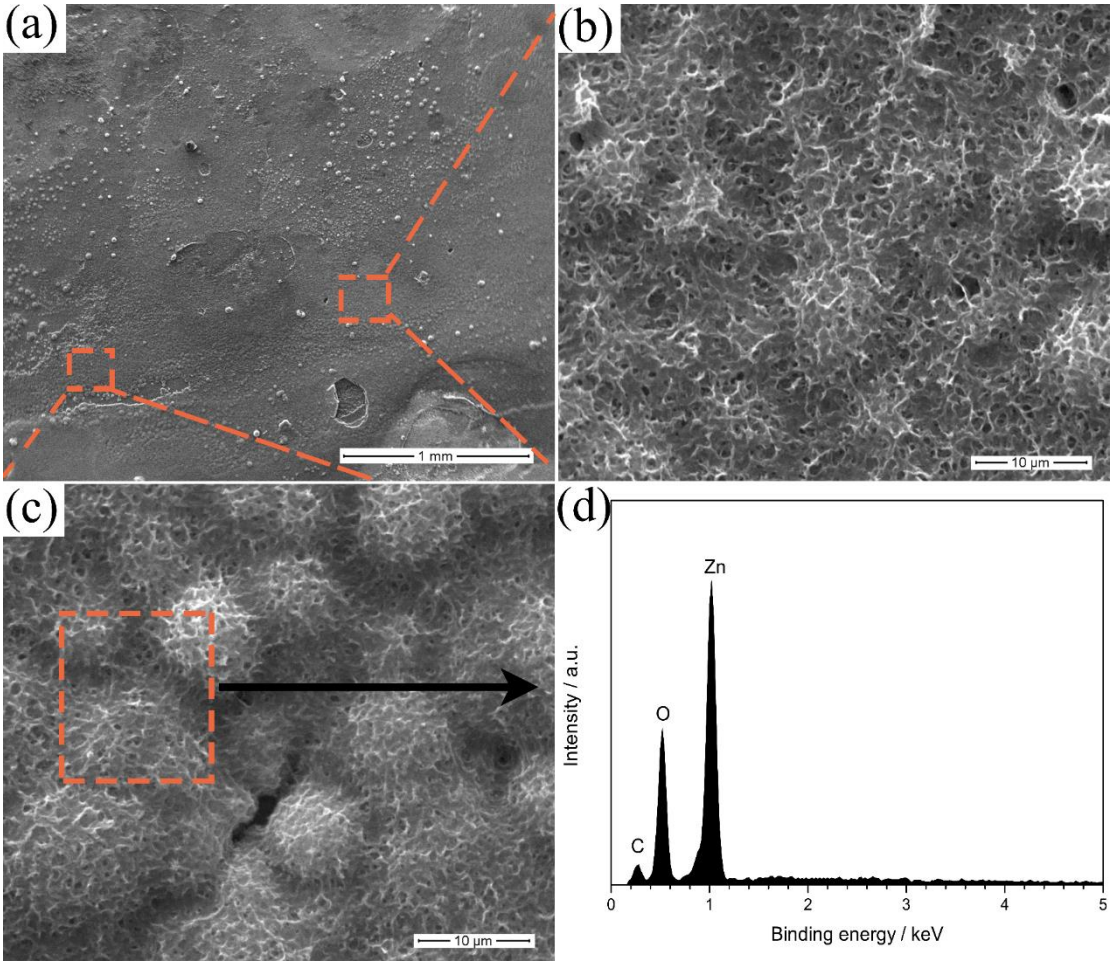

Figure 8. SEM morphology of the corrosion products: a), b) and c) of the Zn coating after 45 days of immersion in 5% NaCl solution, and d) EDS analysis for Fig. 8c

Figure 10 presents the XRD patterns of the corrosion products for the Zn coating and the Zn/Zn-5Al double coating after 45 days of immersion in 5% NaCl solution. The XRD patterns indicate that the corrosion products of the Zn coating mainly consisted of $Zn_5(OH)_8Cl_2 \cdot H_2O$, simonkolleite and a small amount of $Zn(OH)_2$.

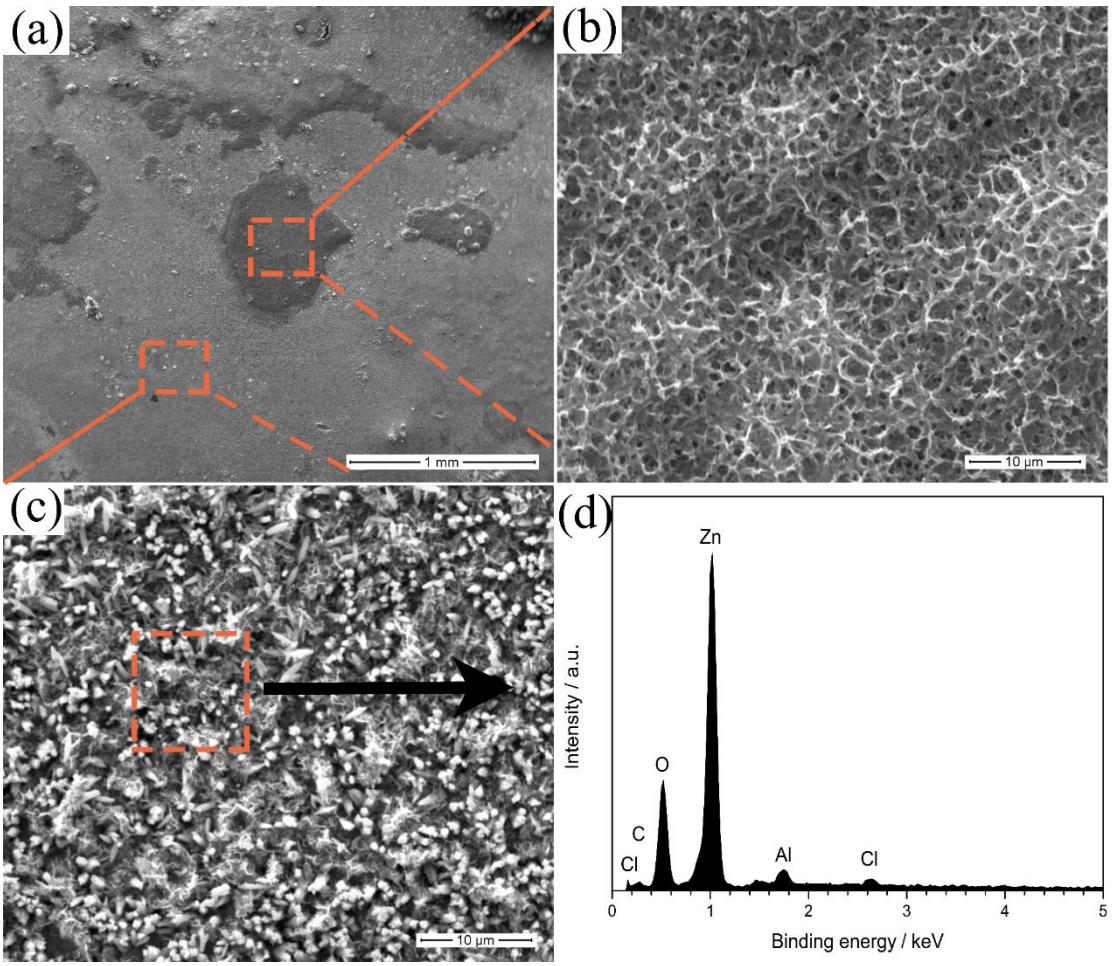

Figure 9. SEM morphology of the corrosion products: a), b) and c) of the Zn/Zn-5Al double coating after 45 days of immersion in 5% NaCl solution, and d) EDS analysis for Fig. 9c

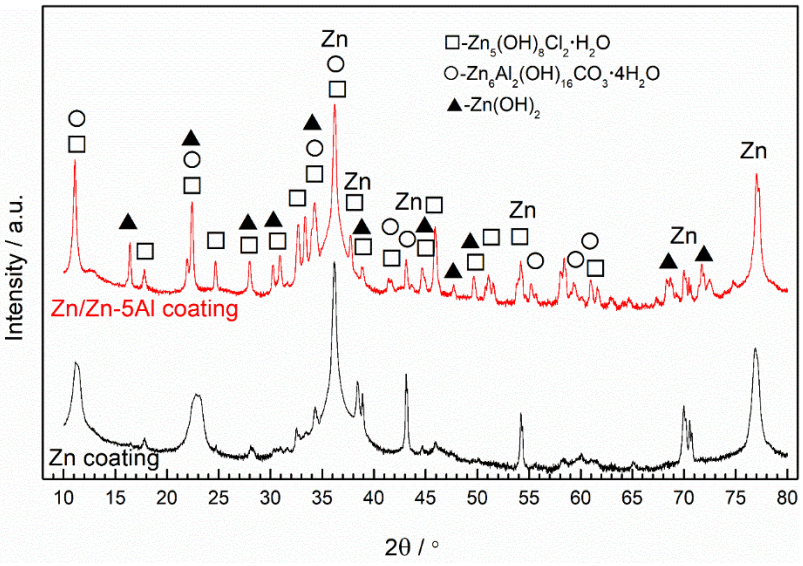

Figure 10. XRD patterns of the corrosion products for the Zn coating and the Zn/Zn-5Al double coating after 45 days of immersion in 5% NaCl solution

The corrosion products of the Zn/Zn-5Al double coating mainly consisted of $Zn_6Al_2(OH)_{16}CO_3 \cdot 4H_2O$, $Zn_5(OH)_8Cl_2 \cdot H_2O$ and $Zn(OH)_2$. This result reveals that the presence of the alloying Al modified the nature of the corrosion products of the double coating compared with the Zn coating.

4. DISCUSSION

As in all coatings, the corrosion resistance of the Zn-5Al coating is dependent on the coating thickness. A maximum thickness of approximately 220 μm for the Zn/Zn-5Al double coating was obtained in this study. Usually, the thickness of a hot-dip Zn-5Al coating is not more than 20 μm. Then, an increase of the Zn-5Al coating is beneficial for prolonging the protection life of the Zn-5Al coating for steel. Figure 1a shows that the Zn/Zn-5Al double coating consisted of a typical coating of Zn on the bottom and a Zn-Al layer on the top. The mass loss test shown in Fig. 2 and the electrochemical study shown in Figs. 5-7 revealed that the corrosion resistance of the Zn/Zn-5Al double coating is 4-5 times larger than that of the Zn coating. This result is consistent with previous studies [11, 16, 18, 19]. The Zn/Zn-5Al double coating not only had a high corrosion resistance that the conventional Zn-5Al coating but also a thicker Zn-5Al layer coupled with the Zn layer on the bottom. To conclude, the new Zn/Zn-5Al double coating obtained in this study can significantly prolong the protection life of the Zn-5Al coating for steel compared with a conventional Zn-5Al coating.

Compared with the SEM morphology of the corrosion products for the Zn coating shown in Fig. 8, the image of the corrosion products for the Zn/Zn-5Al double coating was modified in the presence of the alloying Al. The improved corrosion resistance of the Zn/Zn-5Al double coating compared with the Zn coating was due to the presence of the alloying Al, which could modify the properties of the corrosion products [4, 12-14, 29].

However, the EIS study showed that the corrosion resistance of the Zn/Zn-5Al double coating decreased with prolonged immersion time in 5% NaCl solution. A layer of oxide containing ZnO, Al_2O_3 and $ZnAl_2O_4$ usually covers a hot-dip Zn-Al coating [3, 10, 11, 30]. During the initial corrosion process, due to the barrier effect of the oxide layer on the coating surface, the Zn/Zn-5Al double coating had a higher corrosion resistance. However, with prolonged exposure time, the oxide layer dissolved due to the increase in pH at the corroding interface via reactions [15, 31-33]:

cathodic reaction: $O_2 + 4e^- \; 2H_2O \rightarrow 4OH^-$ (1)

and

$Al_2O_3 + 2OH^- \rightarrow 2AlO_2^- + H_2O$ (2)

Compared with the Zn coating, due to the modification of the corrosion products using the alloying Al, as shown in Figs. 9-10, the Zn/Zn-5Al double coating also had a higher corrosion resistance after a long immersion time in 5% NaCl solution [12, 14, 34].

5. CONCLUSIONS

A new hot dip steel alloy coating with a maximum thickness of approximately 220 μm was obtained in this study. A thicker Zn-5Al coating is beneficial to prolong the protection life of the coating for steel. The neutral salt spray (NSS) test and electrochemical study indicated that the corrosion resistance of the Zn/Zn-5Al double coating was 4-5 times larger than that of the Zn coating. The electrochemical tests also indicated that the corrosion resistance of the Zn-Al coating decreased with immersion time. The double coating had a more negative corrosion potential than that of the Zn-coated steel in 5% NaCl solution. SEM and XRD analyses revealed that the improved corrosion resistance of the Zn/Zn-5Al double coating was mainly attributed to the role of the alloying Al on the corrosion products on the coating surface.

ACKNOWLEDGEMENTS
This investigation was supported by the International Lead and Zinc Research project.

References

1. K.A. Yasakau, S. Kallip, A. Lisenkov, M.G.S. Ferreira, M.L. Zheludkevich, *Electrochim. Acta*, 211 (2016) 126.
2. M.S. Oh, S.H. Kim, J.S. Kim, J.W. Lee, J.H. Shon, Y.S. Jin, *Met. Mater. Int*., 22 (2016) 26.
3. S.M.A. Shibli, B.N. Meena, R. Remya, *Surf. Coat. Technol*., 262 (2015) 210.
4. M.S. Azevedo, C. Allely, K. Ogle, P. Volovitch, *Corros. Sci*., 90 (2015) 482.
5. A. Vimalanandan, A. Bashir, M. Rohwerder, Materials and Corrosion-Werkstoffe Und Korrosion, 65 (2014) 392.
6. E. Diler, B. Rouvellou, S. Rioual, B. Lescop, G.N. Vien, D. Thierry, *Corros. Sci*., 87 (2014) 111.
7. N. LeBozec, D. Thierry, A. Peltola, L. Luxem, G. Luckeneder, G. Marchiaro, M. Rohwerder, *Materials and Corrosion-Werkstoffe Und Korrosion*, 64 (2013) 969.
8. S.R. Yeomans, Galvanized Steel Reinforcement in Concrete, Elsevier, (2004) Amsterdam, Netherlands.
9. Y.Q. Wang, G. Kong, C.S. Che, *Corros. Sci*., 112 (2016) 679.
10. J. Duchoslav, M. Arndt, R. Steinberger, T. Keppert, G. Luckeneder, K.H. Stellnberger, J. Hagler, C.K. Riener, G. Angeli, D. Stifter, *Corros. Sci*., 83 (2014) 327.
11. A. Marder, Prog. Mater. Sci., 45 (2000) 191.
12. X. Zhang, I.O. Wallinder, C. Leygraf, *Surface Engineering*, 34 (2018) 641.
13. J. Stoulil, T. Prosek, A. Nazarov, J. Oswald, P. Kriz, D. Thierry, *Materials and Corrosion-Werkstoffe Und Korrosion*, 66 (2015) 777.
14. P. Volovitch, T.N. Vu, C. Allely, A.A. Aal, K. Ogle, *Corros. Sci*., 53 (2011) 2437.
15. F. Rosalbino, E. Angelini, D. Maccio, A. Saccone, S. Delfino, *Electrochim. Acta,* 54 (2009) 1204.
16. Y. Liu, Z.X. Zhu, Y.X. Chen, B.S. Xu, S.N. Ma, Z.X. Li, Trans. *Nonferrous Met. Soc. China,* 14 (2004) 443.
17. Y.D. He, D.Z. Li, D.R. Wang, Z. Zhang, H.B. Qi, W. Gao, *Mater. Lett*., 56 (2002) 554.
18. H.N. McMurray, G. Parry, B.D. Jeffs, Ironmaking Steelmaking, 25 (1998) 210.
19. H. Katayama, Y.C. Tay, A.S. Viloria, A. Nishikata, T. Tsuru, *Materials Transactions Jim,* 38 (1997) 1089.
20. S.F. Bonabi, F. Ashrafizadeh, A. Sanati, S.M. Nahvi, *J. Therm. Spray Technol*., 27 (2018) 524.
21. E. Tada, Y. Miura, *Isij International,* 56 (2016) 444.

22. T. Prosek, D. Persson, J. Stoulil, D. Thierry, *Corros. Sci*., 86 (2014) 231.
23. H. Katayama, S. Kuroda, *Corros. Sci*., 76 (2013) 35.
24. A.Q. Liu, K. Xiao, C.F. Dong, X.G. Li, *Adv Mater Res-Switz*, 567 (2012) 45.
25. W.J. Zhou, L.K. Xu, J. Wang, N. Li, L.L. Xue, G.Z. Chen, *Acta Metall. Sin.*, 43 (2007) 983.
26. F. Rosalbino, E. Angelini, D. Maccio, A. Saccone, S. Delfino, *Electrochim. Acta*, 52 (2007) 7107.
27. W. Miao, I.S. Cole, A.K. Neufeld, S. Furman, *J. Electrochem. Soc*., 154 (2007) C7.
28. W.R. Osorio, C.M. Freire, A. Garcia, *J. Alloys Compd*., 397 (2005) 179.
29. L.J. Yang, X.D. Zeng, Y.M. Zhang, J. He, Z.L. Song, *Materials and Corrosion-Werkstoffe Und Korrosion,* 66 (2015) 1169.
30. S. Feliu, V. Barranco, *Acta Mater*., 51 (2003) 5413.
31. Z.J. Cao, G. Kong, C.S. Che, Y.Q. Wang, *Appl. Surf. Sci*., 426 (2017) 67.
32. X. Zhang, C. Leygraf, I.O. Wallinder, *Corros. Sci*., 73 (2013) 62.
33. L.J. Yang, Y.M. Zhang, X.D. Zeng, Z.L. Song, *Corros. Sci.*, 59 (2012) 229.
34. T. Ishikawa, M. Ueda, K. Kandori, T. Nakayama, *Corros. Sci*., 49 (2007) 2547.